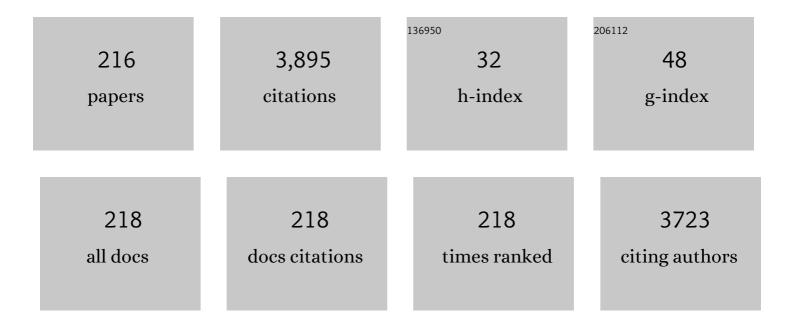
## **Daniel Primetzhofer**

List of Publications by Year in descending order

Source: https://exaly.com/author-pdf/5179271/publications.pdf Version: 2024-02-01



#	Article	IF	CITATIONS
1	Unprecedented severe atomic redistribution in germanium induced by MeV self-irradiation. AIP Advances, 2022, 12, 015209.	1.3	0
2	Synthesis and oxidation behavior of Ti0.35Al0.65By (yÂ=Â1.7–2.4) coatings. Surface and Coatings Technology, 2022, 442, 128190.	4.8	4
3	Energy deposition by H and He ions at keV energies in self-supporting, single crystalline SiC foils. Radiation Physics and Chemistry, 2022, 194, 110033.	2.8	7
4	Ag Surface and Bulk Segregations in Sputtered ZrCuAlNi Metallic Glass Thin Films. Materials, 2022, 15, 1635.	2.9	3
5	Correction to "Influence of Metal Substitution and Ion Energy on Microstructure Evolution of High-Entropy Nitride (TiZrTaMe)N <sub>1–<i>x</i></sub> (Me = Hf, Nb, Mo, or Cr) Films― ACS Applied Electronic Materials, 2022, 4, 1367-1367.	4.3	0
6	Direct Transition from Ultrathin Orthorhombic Dinickel Silicides to Epitaxial Nickel Disilicide Revealed by In Situ Synthesis and Analysis. Small, 2022, 18, 2106093.	10.0	3
7	An in-situ ToF-LEIS and AES study of near-surface modifications of the composition of EUROFER97 induced by thermal annealing, Nuclear Materials and Energy, 2022, 30, 101139. Ab initio-guided X-ray photoelectron spectroscopy quantification of Ti vacancies in Ti <mml:math xmlns:mml="http://www.w3.org/1998/Math/MathML" altimg="si1.svg"&gt;<mml:msub><mml:msub><mml:mrow< td=""><td>1.3</td><td>5</td></mml:mrow<></mml:msub></mml:msub></mml:math 	1.3	5
8	/> <mml:mrow><mml:mn>1</mml:mn><mml:mo>â^'</mml:mo><mml:mi>l´</mml:mi></mml:mrow> xmlns:mml="http://www.w3.org/1998/Math/MathML" altimg="si2.svg"> <mml:mi>l´/&gt;<mml:mi>x</mml:mi>N<mml:math< td=""><td>7.9</td><td>th&gt;O<mml: 2</mml: </td></mml:math<></mml:mi>	7.9	th>O <mml: 2</mml: 
9	xmlns:mml="http://www.w3.org/1998/Math/MathML" altimg="si3.svg"> <mml:msub><mml:mrow .="" acta<br="">M Synthesis of ferromagnetic thin films and engineering of their magnetic properties by Fe ion implantation in polycrystalline Pd. Journal of Magnetism and Magnetic Materials, 2022, 552, 169207.</mml:mrow></mml:msub>	2.3	0
10	Photochromism in Isotopically Labeled Oxygen ontaining Yttriumâ^'Hydride and Deuteride Thinâ€Film Systems. Physica Status Solidi - Rapid Research Letters, 2022, 16, .	2.4	1
11	Oxygen mobility in yttrium hydride films studied by isotopic labelling. EPJ Web of Conferences, 2022, 261, 01001.	0.3	2
12	Ion beam tools for nondestructive in-situ and in-operando composition analysis and modification of materials at the Tandem Laboratory in Uppsala. Journal of Instrumentation, 2022, 17, P04011.	1.2	44
13	Evidence for postnatal neurogenesis in the human amygdala. Communications Biology, 2022, 5, 366.	4.4	18
14	Control of site occupancy by variation of the Zn and Al content in NiZnAl ferrite epitaxial films with low magnetic damping. Physical Review B, 2022, 105, .	3.2	0
15	High Performance Full-Inorganic Flexible Memristor with Combined Resistance-Switching. ACS Applied Materials & Interfaces, 2022, 14, 21173-21180.	8.0	21
16	High-entropy alloy inspired development of compositionally complex superhard (Hf,Ta,Ti,V,Zr)-B-N coatings. Materials and Design, 2022, 218, 110695.	7.0	4
17	Circumventing Thermodynamic Constraints in Nucleation-Controlled Crystallization of Al <sub>2</sub> TiO <sub>5</sub> -Based Chemical Vapor Deposition Coatings. Chemistry of Materials, 2022, 34, 5151-5164.	6.7	2
18	Influence of ion irradiation-induced defects on phase formation and thermal stability of Ti0.27Al0.21N0.52 coatings. Acta Materialia, 2022, 237, 118160.	7.9	7

#	Article	IF	CITATIONS
19	Non-reactive HiPIMS deposition of NbCx thin films: Effect of the target power density on structure-mechanical properties. Surface and Coatings Technology, 2022, 444, 128674.	4.8	7
20	In-situ nanoscale characterization of composition and structure during formation of ultrathin nickel silicide. Applied Surface Science, 2021, 536, 147781.	6.1	8
21	Age hardening in superhard ZrB2-rich Zr1-xTaxBy thin films. Scripta Materialia, 2021, 191, 120-125.	5.2	28
22	Effect of nitrogen vacancies on the growth, dislocation structure, and decomposition of single crystal epitaxial (Ti1-xAlx)Ny thin films. Acta Materialia, 2021, 203, 116509.	7.9	18
23	Hydrogen induced lattice expansion and site occupation analyzed by ion beam methods. Nuclear Instruments & Methods in Physics Research B, 2021, 486, 63-67.	1.4	3
24	Simultaneous assessment of energy, charge state and angular distribution for medium energy ions interacting with ultra-thin self-supporting targets: A time-of-flight approach. Vacuum, 2021, 185, 109988.	3.5	11
25	Orthorhombic Ta3-xN5-yOy thin films grown by unbalanced magnetron sputtering: The role of oxygen on structure, composition, and optical properties. Surface and Coatings Technology, 2021, 406, 126665.	4.8	5
26	P-type cobaltite oxide spinels enable efficient electrocatalytic oxygen evolution reaction. Materials Advances, 2021, 2, 5494-5500.	5.4	2
27	Energy deposition by nonequilibrium charge states of MeV <mml:math xmlns:mml="http://www.w3.org/1998/Math/MathML"&gt; <mml:mmultiscripts> <mml:mi mathvariant="normal"&gt;I <mml:mprescripts></mml:mprescripts> <mml:none /&gt; <mml:mn>127 </mml:mn> </mml:none </mml:mi </mml:mmultiscripts>  in Au, Physical Review A, 2021, 103, .</mml:math 	2.5	7
28	Impact of the experimental approach on the observed electronic energy loss for light keV ions in thin self-supporting films. Nuclear Instruments & Methods in Physics Research B, 2021, 489, 82-87.	1.4	3
29	Determining the chronological sequence of inks deposited with different writing and printing tools using ion beam analysis. Journal of Forensic Sciences, 2021, 66, 1401-1409.	1.6	5
30	Photochromic Response of Encapsulated Oxygenâ€Containing Yttrium Hydride Thin Films. Physica Status Solidi - Rapid Research Letters, 2021, 15, 2000608.	2.4	7
31	Environmental dependence of the photochromic effect of oxygen-containing rare-earth metal hydrides. Journal of Applied Physics, 2021, 129, .	2.5	10
32	Influence of Metal Substitution and Ion Energy on Microstructure Evolution of High-Entropy Nitride (TiZrTaMe)N <sub>1–<i>x</i></sub> (Me = Hf, Nb, Mo, or Cr) Films. ACS Applied Electronic Materials, 2021, 3, 2748-2756.	4.3	8
33	Influence of Ta on the oxidation resistance of WB2â^'z coatings. Journal of Alloys and Compounds, 2021, 864, 158121.	5.5	18
34	Assessing electronic energy loss of heavy ions detected in reflection geometry. Surface and Interface Analysis, 2021, 53, 650.	1.8	2
35	Improving phase stability, hardness, and oxidation resistance of reactively magnetron sputtered (Al,Cr,Nb,Ta,Ti)N thin films by Si-alloying. Surface and Coatings Technology, 2021, 416, 127162.	4.8	31
36	In-situ measurement of diffusion and surface segregation of W and Ta in bare and W-coated EUROFER97 during thermal annealing. Nuclear Materials and Energy, 2021, 27, 100979.	1.3	4

#	Article	IF	CITATIONS
37	Growth of two-dimensional WS2 thin films by reactive sputtering. Vacuum, 2021, 188, 110205.	3.5	14
38	Experimental electronic stopping cross section of tungsten for light ions in a large energy interval. Nuclear Instruments & Methods in Physics Research B, 2021, 498, 1-8.	1.4	8
39	Assessing boron quantification and depth profiling of different boride materials using ion beams. Surface and Coatings Technology, 2021, 417, 127188.	4.8	13
40	Combination of in-situ ion beam analysis and thermal desorption spectroscopy for studying deuterium implanted in tungsten. Physica Scripta, 2021, 96, 124004.	2.5	6
41	Opportunities of combinatorial thin film materials design for the sustainable development of magnesium-based alloys. Scientific Reports, 2021, 11, 17454.	3.3	7
42	Unravelling the ion-energy-dependent structure evolution and its implications for the elastic properties of (V,Al)N thin films. Acta Materialia, 2021, 214, 117003.	7.9	20
43	Interstitial Hydrogen in < mml:math xmlns:mml="http://www.w3.org/1998/Math/MathML" display="inline"> < mml:mrow> < mml:mi> Fe < mml:mo> /  < mml:mi mathvariant="normal">V < /mml:mrow> < /mml:math> Superstructures: Lattice Site Location and Thermal Vibration, Physical Review Letters, 2021, 127, 136102.	7.8	3
44	Assessing the potential of ion beam analytical techniques for depth profiling Li in thin film Li ion batteries. Journal of Applied Physics, 2021, 130, .	2.5	5
45	Multicomponent TixNbCrAl nitride films deposited by dc and high-power impulse magnetron sputtering. Surface and Coatings Technology, 2021, 426, 127743.	4.8	9
46	Mnâ€Rich MnSb <sub>2</sub> Te <sub>4</sub> : A Topological Insulator with Magnetic Gap Closing at High Curie Temperatures of 45–50 K. Advanced Materials, 2021, 33, e2102935.	21.0	70
47	Sensitive in-operando observation of Li and O transport in thin-film Li-ion batteries. Materials Today Energy, 2021, 21, 100844.	4.7	3
48	Magnetron sputtering of carbon supersaturated tungsten films – A chemical approach to increase strength. Materials and Design, 2021, 208, 109874.	7.0	4
49	Enhanced thermal stability of (Ti,Al)N coatings by oxygen incorporation. Acta Materialia, 2021, 218, 117204.	7.9	26
50	Influence of the non-metal species on the oxidation kinetics of Hf, HfN, HfC, and HfB2 coatings. Materials and Design, 2021, 211, 110136.	7.0	22
51	Systematic compositional analysis of sputter-deposited boron-containing thin films. Journal of Vacuum Science and Technology A: Vacuum, Surfaces and Films, 2021, 39, .	2.1	26
52	Direct MoB MBene domain formation in magnetron sputtered MoAlB thin films. Nanoscale, 2021, 13, 18077-18083.	5.6	18
53	Toxicity of stainless and mild steel particles generated from gas–metal arc welding in primary human small airway epithelial cells. Scientific Reports, 2021, 11, 21846.	3.3	4
54	Elemental Depth Profiling of Intact Metal–Organic Framework Single Crystals by Scanning Nuclear Microprobe. Journal of the American Chemical Society, 2021, 143, 18626-18634.	13.7	4

#	Article	IF	CITATIONS
55	Self-Limited Formation of Bowl-Shaped Nanopores for Directional DNA Translocation. ACS Nano, 2021, 15, 17938-17946.	14.6	4
56	The influence of diameter on the magnetic saturation in <mml:math xmlns:mml="http://www.w3.org/1998/Math/MathML" altimg="si9.svg"&gt;<mml:mrow><mml:msub><mml:mrow><mml:mtext>Fe</mml:mtext></mml:mrow><mml:m [0 0 1] multilayered islands. Journal of Magnetism and Magnetic Materials, 2020, 496, 165864.</mml:m </mml:msub></mml:mrow></mml:math 	row> <sup>2:3</sup> ml:ı	mn <sup>2</sup> 84
57	A versatile time-of-flight medium-energy ion scattering setup using multiple delay-line detectors. Nuclear Instruments & Methods in Physics Research B, 2020, 463, 16-20.	1.4	18
58	SIGMA: A Set-up for In-situ Growth, Material modification and Analysis by ion beams. Nuclear Instruments & Methods in Physics Research B, 2020, 463, 96-100.	1.4	11
59	Ion beam analysis of fusion plasma-facing materials and components: facilities and research challenges. Nuclear Fusion, 2020, 60, 025001.	3.5	54
60	Neutralization of slow helium ions scattered from single crystalline aluminum and tantalum surfaces and their oxides. Surface Science, 2020, 691, 121491.	1.9	13
61	Tailoring magnetic order via atomically stacking 3 <i>d</i> /5 <i>d</i> electrons to achieve high-performance spintronic devices. Applied Physics Reviews, 2020, 7, .	11.3	18
62	Photochromism: Photochromic Mechanism and Dualâ€Phase Formation in Oxygenâ€Containing Rareâ€Earth Hydride Thin Films (Advanced Optical Materials 19/2020). Advanced Optical Materials, 2020, 8, 2070078.	7.3	1
63	Assessing electron emission induced by pulsed ion beams: A time-of-flight approach. Nuclear Instruments & Methods in Physics Research B, 2020, 479, 217-221.	1.4	7
64	Contrast modes in a 3D ion transmission approach at keV energies. Ultramicroscopy, 2020, 217, 113051.	1.9	7
65	Effect of nitrogen content on microstructure and corrosion resistance of sputter-deposited multicomponent (TiNbZrTa)Nx films. Surface and Coatings Technology, 2020, 404, 126485.	4.8	16
66	Thermal stability and mechanical properties of sputtered (Hf,Ta,V,W,Zr)-diborides. Acta Materialia, 2020, 200, 559-569.	7.9	50
67	Correlation between fracture characteristics and valence electron concentration of sputtered Hf-C-N based thin films. Surface and Coatings Technology, 2020, 399, 126212.	4.8	18
68	Electrochromism in Ni Oxide Thin Films Made by Advanced Gas Deposition and Sputtering: A Comparative Study Demonstrating the Significance of Surface Effects. Journal of the Electrochemical Society, 2020, 167, 116519.	2.9	4
69	<i>In-operando</i> observation of Li depth distribution and Li transport in thin film Li ion batteries. Applied Physics Letters, 2020, 117, .	3.3	13
70	In-situ characterization of ultrathin nickel silicides using 3D medium-energy ion scattering. Scientific Reports, 2020, 10, 10249.	3.3	3
71	A Proposal for a Composite with Temperature-Independent Thermophysical Properties: HfV2–HfV2O7. Materials, 2020, 13, 5021.	2.9	4
72	Trajectory-dependent electronic excitations by light and heavy ions around and below the Bohr velocity. Physical Review A, 2020, 102, .	2.5	20

#	Article	IF	CITATIONS
73	Preferential Orientation of Photochromic Gadolinium Oxyhydride Films. Molecules, 2020, 25, 3181.	3.8	9
74	Influence of structure and cation distribution on magnetic anisotropy and damping in Zn/Al doped nickel ferrites. Physical Review B, 2020, 102, .	3.2	14
75	Experimental electronic stopping cross section of transition metals for light ions: Systematics around the stopping maximum. Physical Review A, 2020, 102, .	2.5	18
76	Correlating chemical composition and optical properties of photochromic rare-earth oxyhydrides using ion beam analysis. Nuclear Instruments & Methods in Physics Research B, 2020, 485, 36-40.	1.4	18
77	Boron Concentration Induced Co-Ta-B Composite Formation Observed in the Transition from Metallic to Covalent Glasses. Condensed Matter, 2020, 5, 18.	1.8	1
78	Solar wind Helium ion interaction with Mg and Fe rich pyroxene as Mercury surface analogue. Nuclear Instruments & Methods in Physics Research B, 2020, 480, 10-15.	1.4	9
79	Electronic excitation of transition metal nitrides by light ions with keV energies. Journal of Physics Condensed Matter, 2020, 32, 405502.	1.8	1
80	Disparate Energy Scaling of Trajectory-Dependent Electronic Excitations for Slow Protons and He Ions. Physical Review Letters, 2020, 124, 096601.	7.8	42
81	Oxidation behaviour of V2AlC MAX phase coatings. Journal of the European Ceramic Society, 2020, 40, 4436-4444.	5.7	33
82	Synthesis and in-situ characterization of photochromic yttrium oxyhydride grown by reactive eâ^'-beam evaporation. Scripta Materialia, 2020, 186, 352-356.	5.2	15
83	Photoluminescence enhancement and high accuracy patterning of lead halide perovskite single crystals by MeV ion beam irradiation. Journal of Materials Chemistry C, 2020, 8, 9923-9930.	5.5	12
84	A multipurpose set-up using keV ions for nuclear reaction analysis, high-resolution backscattering spectrometry, low-energy PIXE and in-situ irradiation experiments. Nuclear Instruments & Methods in Physics Research B, 2020, 478, 104-110.	1.4	7
85	Dynamic Potential Sputtering of Lunar Analog Material by Solar Wind Ions. Astrophysical Journal, 2020, 891, 100.	4.5	22
86	Spinodal decomposition of reactively sputtered (V0.64Al0.36)0.49N0.51 thin films. Surface and Coatings Technology, 2020, 389, 125641.	4.8	11
87	Low temperature oxidation behavior of Mo2BC coatings. Journal of Vacuum Science and Technology A: Vacuum, Surfaces and Films, 2020, 38, 023403.	2.1	1
88	Photochromic Mechanism and Dualâ€Phase Formation in Oxygenâ€Containing Rareâ€Earth Hydride Thin Films. Advanced Optical Materials, 2020, 8, 2000822.	7.3	15
89	Stress-dependent prediction of metastable phase formation for magnetron-sputtered V1â^'xAlxN and Ti1â''xAlxN thin films. Acta Materialia, 2020, 196, 313-324.	7.9	20
90	Electrochromism of nitrogen-doped tungsten oxide thin films. Materials Today: Proceedings, 2020, 33, 2434-2439.	1.8	5

#	Article	IF	CITATIONS
91	Nonreciprocal spin pumping damping in asymmetric magnetic trilayers. Physical Review B, 2020, 101, .	3.2	13
92	Large room temperature relative cooling power in La0.5Pr0.2Ca0.1Sr0.2MnO3. Journal of Alloys and Compounds, 2020, 827, 154292.	5.5	18
93	Photochromic properties of yttrium oxyhydride thin films: Surface versus bulk effect. Materialia, 2020, 11, 100706.	2.7	16
94	On the influence of uncertainties in scattering potentials on quantitative analysis using keV ions. Nuclear Instruments & Methods in Physics Research B, 2020, 470, 21-27.	1.4	6
95	The influence of pressure and magnetic field on the deposition of epitaxial TiBx thin films from DC magnetron sputtering. Vacuum, 2020, 177, 109355.	3.5	14
96	Experimental Insights Into Space Weathering of Phobos: Laboratory Investigation of Sputtering by Atomic and Molecular Planetary Ions. Journal of Geophysical Research E: Planets, 2020, 125, e2020JE006583.	3.6	15
97	Accurate high-resolution depth profiling of magnetron sputtered transition metal alloy films containing light species: A multi-method approach. Thin Solid Films, 2019, 686, 137416.	1.8	46
98	Hydrogen site location in ultrathin vanadium layers by N-15 nuclear reaction analysis. Nuclear Instruments & Methods in Physics Research B, 2019, 455, 57-60.	1.4	3
99	Phase composition and transformations in magnetron-sputtered (Al,V)2O3 coatings. Thin Solid Films, 2019, 688, 137369.	1.8	4
100	Ion energy control via the electrical asymmetry effect to tune coating properties in reactive radio frequency sputtering. Plasma Sources Science and Technology, 2019, 28, 114001.	3.1	22
101	Synthesis and Properties of Orthorhombic MoAlB Coatings. Coatings, 2019, 9, 510.	2.6	17
102	Antimonyâ€Doped Tin Oxide as Transparent Back Contact in Cu 2 ZnSnS 4 Thinâ€Film Solar Cells. Physica Status Solidi (A) Applications and Materials Science, 2019, 216, 1900542.	1.8	3
103	Electronic interaction of slow hydrogen and helium ions with nickel-silicon systems. Physical Review A, 2019, 100, .	2.5	16
104	Aggregation of Au( <scp>i</scp> )-complexes on amorphous substrates governed by aurophilicity. Dalton Transactions, 2019, 48, 14712-14723.	3.3	5
105	In-situ composition analysis of photochromic yttrium oxy-hydride thin films under light illumination. Solar Energy Materials and Solar Cells, 2019, 201, 110119.	6.2	15
106	Stress-Dependent Elasticity of TiAlN Coatings. Coatings, 2019, 9, 24.	2.6	20
107	On the Z1-dependence of electronic stopping in TiN. Scientific Reports, 2019, 9, 176.	3.3	12
108	Electrochromic WO <sub>3</sub> thin films attain unprecedented durability by potentiostatic pretreatment. Journal of Materials Chemistry A, 2019, 7, 2908-2918.	10.3	66

#	Article	IF	CITATIONS
109	Remote Tracking of Phase Changes in Cr2AlC Thin Films by In-situ Resistivity Measurements. Scientific Reports, 2019, 9, 8266.	3.3	28
110	Overview of the JET preparation for deuterium–tritium operation with the ITER like-wall. Nuclear Fusion, 2019, 59, 112021.	3.5	87
111	Enhanced Gilbert damping in Re-doped FeCo films: Combined experimental and theoretical study. Physical Review B, 2019, 99, .	3.2	5
112	Atomic layer deposition of amorphous tin-gallium oxide films. Journal of Vacuum Science and Technology A: Vacuum, Surfaces and Films, 2019, 37, 030906.	2.1	14
113	Investigation of the energy loss of I in Au at energies below the Bragg peak. Nuclear Instruments & Methods in Physics Research B, 2019, 450, 37-42.	1.4	5
114	Correlative Experimental and Theoretical Investigation of the Angle-Resolved Composition Evolution of Thin Films Sputtered from a Compound Mo2BC Target. Coatings, 2019, 9, 206.	2.6	10
115	Ion-beam based characterization of TiN back contact interlayers for CZTS(e) thin film solar cells. Nuclear Instruments & Methods in Physics Research B, 2019, 450, 262-266.	1.4	1
116	Modeling of metastable phase formation for sputtered Ti1-xAlxN thin films. Acta Materialia, 2019, 165, 615-625.	7.9	34
117	The impact of surface oxidation on energy spectra of keV ions scattered from transition metals. Applied Surface Science, 2019, 479, 1287-1292.	6.1	10
118	A note on extracting electronic stopping from energy spectra of backscattered slow ions applying Bragg's rule. Nuclear Instruments & Methods in Physics Research B, 2018, 423, 82-86.	1.4	13
119	Stopping cross section of vanadium for H + and He + ions in a large energy interval deduced from backscattering spectra. Nuclear Instruments & Methods in Physics Research B, 2018, 424, 43-51.	1.4	16
120	Modifying the nanostructure and the mechanical properties of Mo2BC hard coatings: Influence of substrate temperature during magnetron sputtering. Materials and Design, 2018, 142, 203-211.	7.0	16
121	Ion-induced particle desorption in time-of-flight medium energy ion scattering. Nuclear Instruments & Methods in Physics Research B, 2018, 423, 22-26.	1.4	6
122	Influence of carbon deficiency on phase formation and thermal stability of super-hard TaCy thin films. Scripta Materialia, 2018, 149, 150-154.	5.2	25
123	Composition of photochromic oxygen-containing yttrium hydride films. Solar Energy Materials and Solar Cells, 2018, 177, 66-69.	6.2	27
124	Impact of Hâ€Uptake from Forming Gas Annealing and Ion Implantation on the Photoluminescence of Si Nanoparticles. Physica Status Solidi (A) Applications and Materials Science, 2018, 215, 1700444.	1.8	0
125	Analysis of photon emission induced by light and heavy ions in time-of-flight medium energy ion scattering. Nuclear Instruments & Methods in Physics Research B, 2018, 417, 75-80.	1.4	7
126	Reference binding energies of transition metal carbides by core-level x-ray photoelectron spectroscopy free from Ar+ etching artefacts. Applied Surface Science, 2018, 436, 102-110.	6.1	68

8

#	Article	IF	CITATIONS
127	Tuning structure and mechanical properties of Ta-C coatings by N-alloying and vacancy population. Scientific Reports, 2018, 8, 17669.	3.3	27
128	TiN Interlayers with Varied Thickness in Cu <sub>2</sub> ZnSnS(e) <sub>4</sub> Thin Film Solar Cells: Effect on Na Diffusion, Back Contact Stability, and Performance. Physica Status Solidi (A) Applications and Materials Science, 2018, 215, 1800491.	1.8	13
129	Sputtering of polished EUROFER97 steel: Surface structure modification and enrichment with tungsten and tantalum. Journal of Nuclear Materials, 2018, 508, 139-146.	2.7	16
130	Luminescence of silicon nanoparticles from oxygen implanted silicon. Materials Science in Semiconductor Processing, 2018, 86, 18-22.	4.0	2
131	Cation…Anionâ€Based Electrochemical Degradation and Rejuvenation of Electrochromic Nickel Oxide Thin Films. ChemElectroChem, 2018, 5, 3548-3556.	3.4	10
132	Substoichiometry and tantalum dependent thermal stability of α-structured W-Ta-B thin films. Scripta Materialia, 2018, 155, 5-10.	5.2	38
133	Yttrium oxyhydrides for photochromic applications: Correlating composition and optical response. Physical Review Materials, 2018, 2, .	2.4	29
134	Formation of nickel germanides from Ni layers with thickness below 10 nm. Journal of Vacuum Science and Technology B:Nanotechnology and Microelectronics, 2017, 35, 020602.	1.2	4
135	Elastic properties of amorphousT0.75Y0.75B14(T  =  Sc, Ti, V, Y, Zr, Nb) and the effect of O inc on bonding, density and elasticity (T′  =  Ti, Zr). Journal of Physics Condensed Matter, 2017,	orpgratior 29, 0854	ו 24.
136	Electronic Stopping of Slow Protons in Transition and Rare Earth Metals: Breakdown of the Free Electron Gas Concept. Physical Review Letters, 2017, 118, 103401.	7.8	52
137	Unprecedented Al supersaturation in single-phase rock salt structure VAIN films by Al+ subplantation. Journal of Applied Physics, 2017, 121, .	2.5	40
138	Characterization of compositional modifications in metal-organic frameworks using carbon and alpha particle microbeams. Nuclear Instruments & Methods in Physics Research B, 2017, 404, 198-201.	1.4	2
139	Enhanced photochromic response in oxygen-containing yttrium hydride thin films transformed by an oxidation process. Solar Energy Materials and Solar Cells, 2017, 166, 185-189.	6.2	23
140	Uniform distribution of post-synthetic linker exchange in metal–organic frameworks revealed by Rutherford backscattering spectrometry. Chemical Communications, 2017, 53, 6516-6519.	4.1	27
141	Compositional and morphological analysis of FeW films modified by sputtering and heating. Nuclear Materials and Energy, 2017, 12, 472-477.	1.3	10
142	A Solutionâ€Doped Polymer Semiconductor:Insulator Blend for Thermoelectrics. Advanced Science, 2017, 4, 1600203.	11.2	72
143	Electronic energy-loss mechanisms for H, He, and Ne in TiN. Physical Review A, 2017, 96, .	2.5	20
144	Characterization of TiN back contact interlayers with varied thickness for Cu 2 ZnSn(S,Se) 4 thin film solar cells. Thin Solid Films, 2017, 639, 91-97.	1.8	15

#	Article	IF	CITATIONS
145	HPPMS deposition from composite targets: Effect of two orders of magnitude target power density changes on the composition of sputtered Cr-Al-C thin films. Vacuum, 2017, 145, 285-289.	3.5	20
146	Influence of swift heavy ion irradiation on the photoluminescence of Si-nanoparticles and defects in SiO2. Nanotechnology, 2017, 28, 375603.	2.6	7
147	Electrochemical Rejuvenation of Anodically Coloring Electrochromic Nickel Oxide Thin Films. ACS Applied Materials & Interfaces, 2017, 9, 42420-42424.	8.0	61
148	Electronic Stopping of Slow Protons in Oxides: Scaling Properties. Physical Review Letters, 2017, 119, 163401.	7.8	34
149	Core-level spectra and binding energies of transition metal nitrides by non-destructive x-ray photoelectron spectroscopy through capping layers. Applied Surface Science, 2017, 396, 347-358.	6.1	109
150	Phase formation of Nb2AlC investigated by combinatorial thin film synthesis and ab initio calculations. Journal of the European Ceramic Society, 2017, 37, 35-41.	5.7	7
151	Unprecedented thermal stability of inherently metastable titanium aluminum nitride by point defect engineering. Materials Research Letters, 2017, 5, 158-169.	8.7	73
152	Non-reactively sputtered ultra-high temperature Hf-C and Ta-C coatings. Surface and Coatings Technology, 2017, 309, 436-444.	4.8	35
153	Massive Ta diffusion observed in Cu thin films but not in Ag counterparts. Journal of Vacuum Science and Technology B:Nanotechnology and Microelectronics, 2016, 34, .	1.2	3
154	Structural, mechanical, and magnetic properties of GaFe3N thin films. Journal of Vacuum Science and Technology A: Vacuum, Surfaces and Films, 2016, 34, 040601.	2.1	3
155	MeV ion irradiation effects on the luminescence properties of Si-implanted SiO2 -thin films. Physica Status Solidi C: Current Topics in Solid State Physics, 2016, 13, 921-926.	0.8	1
156	Correlative theoretical and experimental investigation of the formation of AlYB14 and competing phases. Journal of Applied Physics, 2016, 119, .	2.5	6
157	Substrate rotation-induced chemical modulation in Ti-Al-O-N coatings synthesized by cathodic arc in an industrial deposition plant. Surface and Coatings Technology, 2016, 305, 249-253.	4.8	30
158	Ferroelectric phase transitions in multiferroicGe1â^'xMnxTedriven by local lattice distortions. Physical Review B, 2016, 94, .	3.2	13
159	Epitaxial and textured TiN thin films grown on MgO(1 0 0) by reactive HiPIMS: the impact of charging on epitaxial to textured growth crossover. Journal Physics D: Applied Physics, 2016, 49, 455301.	2.8	5
160	Ion beam analysis of tungsten layers in EUROFER model systems and carbon plasma facing components. Nuclear Instruments & Methods in Physics Research B, 2016, 371, 355-359.	1.4	11
161	Energy loss of slow Ne ions in Pt and Ag from TOF-MEIS and Monte-Carlo simulations. Nuclear Instruments & Methods in Physics Research B, 2016, 371, 76-80.	1.4	9
162	The potential of ion beams for characterization of metal–organic frameworks. Nuclear Instruments & Methods in Physics Research B, 2016, 371, 327-331.	1.4	3

#	Article	IF	CITATIONS
163	Composition driven phase evolution and mechanical properties of Mo–Cr–N hard coatings. Journal of Applied Physics, 2015, 118, .	2.5	34
164	Si-nanoparticle synthesis using ion implantation and MeV ion irradiation. Physica Status Solidi C: Current Topics in Solid State Physics, 2015, 12, 1301-1305.	0.8	6
165	Galvanostatic Ion Detrapping Rejuvenates Oxide Thin Films. ACS Applied Materials & Interfaces, 2015, 7, 26387-26390.	8.0	77
166	Characterization of high-k dielectrics using MeV elastic scattering of He ions. Nuclear Instruments & Methods in Physics Research B, 2015, 347, 52-57.	1.4	2
167	Characterization of magnetron sputtered Cr–B and Cr–B–C thin films for electrical contact applications. Surface and Coatings Technology, 2015, 266, 167-176.	4.8	40
168	Vacancy filling effect in thermoelectric NbO. Journal of Physics Condensed Matter, 2015, 27, 115501.	1.8	10
169	Development of W–SiO2 and Nb–TiO2 solar absorber coatings for combined heat and power systems at intermediate operation temperatures. Solar Energy Materials and Solar Cells, 2015, 133, 180-193.	6.2	33
170	Effect of oxygen incorporation on the structure and elasticity of Ti-Al-O-N coatings synthesized by cathodic arc and high power pulsed magnetron sputtering. Journal of Applied Physics, 2014, 116, .	2.5	51
171	Crystal Phase Transitions in the Shell of PbS/CdS Core/Shell Nanocrystals Influences Photoluminescence Intensity. Chemistry of Materials, 2014, 26, 5914-5922.	6.7	44
172	Electronic interactions of medium-energy ions in hafnium dioxide. Physical Review A, 2014, 89, .	2.5	9
173	ToF-MEIS stopping measurements in thin SiC films. Nuclear Instruments & Methods in Physics Research B, 2014, 332, 130-133.	1.4	4
174	The potential of Rutherford Backscattering Spectrometry for composition analysis of colloidal nanocrystals. Nuclear Instruments & Methods in Physics Research B, 2014, 332, 122-125.	1.4	2
175	Electronic stopping power of hydrogen in HfO2 at the stopping maximum and below. Nuclear Instruments & Methods in Physics Research B, 2014, 320, 100-103.	1.4	14
176	Tuning the Localized Surface Plasmon Resonance in Cu <sub>2–<i>x</i></sub> Se Nanocrystals by Postsynthetic Ligand Exchange. ACS Applied Materials & Interfaces, 2014, 6, 17770-17775.	8.0	68
177	Ion-stimulated desorption in the medium-energy regime. Japanese Journal of Applied Physics, 2014, 53, 060305.	1.5	2
178	Electrical properties of Ag/Ta and Ag/TaN thin-films. Microelectronic Engineering, 2014, 120, 257-261.	2.4	7
179	Ultra-thin film and interface analysis of high-k dielectric materials employing Time-Of-Flight Medium Energy Ion Scattering (TOF-MEIS). Nuclear Instruments & Methods in Physics Research B, 2014, 332, 212-215.	1.4	8
180	Matrix effects in the neutralization of He ions at a metal surface containing oxygen. Surface Science, 2013, 609, 167-171.	1.9	17

#	Article	IF	CITATIONS
181	Effects of the atomic level shift in the Auger neutralization rates of noble metal surfaces. Nuclear Instruments & Methods in Physics Research B, 2013, 315, 206-212.	1.4	11
182	Electronic stopping power of slow 20Ne ions in Au obtained from TOF-MEIS and Monte-Carlo computer simulations. Nuclear Instruments & Methods in Physics Research B, 2013, 315, 26-29.	1.4	6
183	Local vs. non-local energy loss of low energy ions: Influence of charge exchange processes in close collisions. Nuclear Instruments & Methods in Physics Research B, 2013, 317, 8-12.	1.4	12
184	A procedure to determine electronic energy loss from relative measurements with TOF-LEIS. Nuclear Instruments & Methods in Physics Research B, 2013, 317, 61-65.	1.4	25
185	Auger neutralization of He+ on Cu surfaces: Simulation of azimuthal scans. Nuclear Instruments & Methods in Physics Research B, 2013, 317, 23-27.	1.4	4
186	Analysis of Mo/Si multilayers by means of RBS. Nuclear Instruments & Methods in Physics Research B, 2013, 317, 126-129.	1.4	5
187	Tuning the Magnetic Properties of Metal Oxide Nanocrystal Heterostructures by Cation Exchange. Nano Letters, 2013, 13, 586-593.	9.1	91
188	Quasi-resonant neutralization of He <sup>+</sup> ions at a germanium surface. Journal of Physics Condensed Matter, 2013, 25, 485006.	1.8	10
189	Bandgap widening in thermochromic Mg-doped VO2 thin films: Quantitative data based on optical absorption. Applied Physics Letters, 2013, 103, .	3.3	72
190	New beam line for time-of-flight medium energy ion scattering with large area position sensitive detector. Review of Scientific Instruments, 2012, 83, 095107.	1.3	57
191	Inelastic energy loss of medium energy H and He ions in Au and Pt: Deviations from velocity proportionality. Physical Review B, 2012, 86, .	3.2	32
192	Electronic Excitations of Slow Ions in a Free Electron Gas Metal: Evidence for Charge Exchange Effects. Physical Review Letters, 2011, 107, 163201.	7.8	64
193	Resonant charge transfer in low-energy ion scattering: Information depth in the reionization regime. Surface Science, 2011, 605, 1913-1917.	1.9	28
194	Electronic stopping power of hydrogen in KCl at the stopping maximum and at very low energies. Nuclear Instruments & Methods in Physics Research B, 2011, 269, 2063-2066.	1.4	7
195	Influence of screening length modification on the scattering cross section in LEIS. Nuclear Instruments & Methods in Physics Research B, 2011, 269, 1292-1295.	1.4	10
196	Trace element quantification in high-resolution Rutherford backscattering spectrometry. Nuclear Instruments & Methods in Physics Research B, 2011, 269, 1284-1287.	1.4	15
197	Calculation of Auger-neutralization probabilities for He+-ions in LEIS. Nuclear Instruments & Methods in Physics Research B, 2011, 269, 1296-1299.	1.4	11
198	Charge exchange of He+-ions with aluminium surfaces. Nuclear Instruments & Methods in Physics Research B, 2011, 269, 1171-1174.	1.4	21

#	Article	IF	CITATIONS
199	Simulation of energy spectra of slow He+ ions scattered from a copper surface. Nuclear Instruments & Methods in Physics Research B, 2011, 269, 1425-1427.	1.4	2
200	Growth and optical properties of Ag clusters deposited on poly(ethylene terephthalate). Nanotechnology, 2011, 22, 275710.	2.6	8
201	Band structure effects in Auger neutralization of He ions at metal surfaces. Physical Review B, 2011, 84, .	3.2	21
202	A study of a LEIS azimuthal scan behavior: Classical dynamics simulation. Surface Science, 2010, 604, 1906-1911.	1.9	6
203	xmlns:mml="http://www.w3.org/1998/Math/MathML" display="inline"> <mml:mrow><mml:msup><mml:mrow><mml:mmultiscripts><mml:mtext>H</mml:mtext><mm /&gt;<mml:none /&gt;<mml:mn>4</mml:mn></mml:none </mm </mml:mmultiscripts><mml:mtext>e</mml:mtext></mml:mrow><mml:mo>+<td>0.2</td><td></td></mml:mo></mml:msup></mml:mrow>	0.2	
204	scattered from noble metals and alloy surfaces. Physical Review B, 2009, 80, . Electronic stopping of low-energy H and He in Cu and Au investigated by time-of-flight low-energy ion scattering. Physical Review B, 2009, 80, .	3.2	76
205	Vanishing Electronic Energy Loss of Very Slow Light Ions in Insulators with Large Band Gaps. Physical Review Letters, 2009, 103, 113201.	7.8	82
206	LEIS: A reliable tool for surface composition analysis?. Nuclear Instruments & Methods in Physics Research B, 2009, 267, 624-627.	1.4	12
207	Azimuthal scans in LEIS: Influence of the scattering potential. Nuclear Instruments & Methods in Physics Research B, 2009, 267, 638-641.	1.4	3
208	Analysis of the Auger neutralization of He+ at Cu surfaces in low energy ion scattering. Nuclear Instruments & Methods in Physics Research B, 2009, 267, 575-577.	1.4	3
209	On the origin of the LEIS signal in TOF- and in ESA-LEIS. Nuclear Instruments & Methods in Physics Research B, 2009, 267, 634-637.	1.4	7
210	Strength of the interatomic potential derived from angular scans in LEIS. Surface Science, 2008, 602, 2921-2926.	1.9	24
211	Electronic interaction of very slow light ions in Au: Electronic stopping and electron emission. Physical Review B, 2008, 78, .	3.2	55
212	Quantitative analysis of ultra thin layer growth by time-of-flight low energy ion scattering. Applied Physics Letters, 2008, 92, .	3.3	17
213	Crystal Effects in the Neutralization of <mml:math <br="" xmlns:mml="http://www.w3.org/1998/Math/MathML">display="inline"&gt;<mml:msup><mml:mi>He</mml:mi><mml:mo>+</mml:mo></mml:msup></mml:math> Ions in the Low Energy Ion Scattering Regime. Physical Review Letters, 2008, 100, 213201.	7.8	31
214	Neutralization of low energy He+ ions by Cu in the Auger regime. Nuclear Instruments & Methods in Physics Research B, 2007, 258, 18-20.	1.4	5
215	Influence of screening and electronic stopping on LEIS spectra. Nuclear Instruments & Methods in Physics Research B, 2007, 258, 32-35.	1.4	5
216	On the surface sensitivity of angular scans in LEIS. Nuclear Instruments & Methods in Physics Research B, 2007, 258, 36-39.	1.4	14